Pilot Design for OFDM with Null Edge Subcarriers

Robert J. Baxley, John E. Kleider, and G. Tong Zhou

***Abstract*—Pilot symbol assisted modulation (PSAM) orthogonal frequency division multiplexing (OFDM) has proven to be a popular technique for high-speed communication through multipath fading channels. In this paper we examine PSAM pilot design optimization in OFDM systems that employ edge null subcarriers for spectral shaping. Specifically, we show that the commonly used even pilot spacing design is suboptimal in terms of symbol estimate mean squared error (MSE) performance when a sufficient number of null subcarriers are present. We pursue a parametric design of the pilot spacings and use convex optimization techniques in order to find a pilot design that results in near-optimal symbol estimate MSE performance. Finally, we present several example PSAM OFDM pilot designs including one example based on the IEEE 802.16 standard to demonstrate performance improvements over the conventional even-spacing pilot design when null edge subcarriers are present.**

***Index Terms*—Orthogonal frequency division multiplexing (OFDM), pilot symbol assisted modulation (PSAM).**

I. Introduction

ORTHOGONAL frequency division multiplexing (OFDM) is a popular method in wireless high-speed communications schemes [2]. Pilot symbol assisted modulation (PSAM) was proposed as a low complexity technique to estimate multipath channels and to remove their effects from the received OFDM symbol [3]. More recently, attention has been paid to optimal pilot design for channel estimation performance in OFDM. In [4], it was demonstrated that the mean squared error (MSE) minimizing pilot design consists of equi-spaced equi-powered pilots. Other pilot design criteria have been considered as well: in [5] for bit error rate (BER) minimization, in [6] for channel estimate MSE minimization, in [7] for multiple-input multiple-output (MIMO) preamble pilot design, in [8] for channel tracking performance, in [9] for Doppler spread mitigation, in [10] for channel capacity maximization, in [11] for multiuser pilot design, in [12] for MIMO channel capacity maximization, in [13] for MIMO channel estimate MSE minimization, and in [14]–[16] for peak-to-average power ratio (PAR) reduction. A thorough overview of PSAM can be found in [17]. In this paper, we will address optimal pilot designs in ODFM systems that have edge null subcarriers.

In almost all wireless communications standards, the transmitted signal is required to meet a spectral mask such that the power spectrum outside of the main user's channel is not too high, thus limiting the amount of distortion noise contributed to adjacent and alternate channel users. Such interference results from spectral splattering caused by system nonlinearities from the power amplifier, the mixer, the DAC, etc. Accordingly, many OFDM standards (digital audio broadcasting (DAB), digital video broadcasting (DVB), wireless LAN, wireless MAN, etc.) require that a certain number of subcarriers at each band edge remain unmodulated. These unmodulated (or "null") subcarriers make it easier for system designers to meet the spectral mask constraints [18]. As we will show, when a segment of the bandwidth is not available for pilot placement, as is the case in null-subcarrier OFDM systems, the pilot design problem needs to be carefully considered.

When the entire OFDM band is available (i.e., no null subcarriers are present), it was proved in [4] that the optimal pilot design consists of evenly-spaced constant-power pilots. In this work we are interested in determining the optimal pilot design when null edge subcarriers are present. If the null subcarriers occupy a larger bandwidth than the spacing required by the evenly-spaced pilot design, then evenly spacing the pilot subcarriers is no longer feasible, and another solution needs to be found as acknowledged in [4] and [6]. Also, in [19], a proposal was made for selecting the pilot positions in OFDM preambles when null subcarriers are present. However, the method of [19] does not work for certain subcarrier/channel-length configurations; moreover, the optimization in [19] uses the ℓ_2 norm of the subcarrier channel-estimate MSEs, which may not accurately encapsulate the system performance.

Our proposed solution uses a cubic parameterization of the pilot subcarrriers in conjunction with a convex optimization algorithm to produce pilot designs that have near-optimal *symbol* estimate MSE performance as defined by *any* convex norm of the subcarrier symbol-estimate MSEs. In the example designs we show the effect of using different norm choices. Additionally, through a design example based on the IEEE 802.16 standard [20], we demonstrate the performance improvement possible for null-subcarrier OFDM systems when the proposed pilot design is used instead of the conventional evenly-spaced pilot design.

Notations: Upper case and lower case bold face letters represent matrices and column vectors respectively; $\mathbf{A}^T$ and $\mathbf{A}^{\mathcal{H}}$ stand for the transpose and the Hermitian transpose of

Manuscript received January 16, 2008; revised July 9, 2008; accepted September 5, 2008. The associate editor coordinating the review of this paper and approving it for publication was D. Huang.

R. J. Baxley is with the Georgia Tech Research Institute, Atlanta, GA 30332-0817, USA (e-mail: bob.baxley@gtri.gatech.edu).

G. T. Zhou is with the School of Electrical and Computer Engineering, Georgia Institute of Technology, Atlanta, GA 30332-0250, USA (e-mail: gtz@ece.gatech.edu).

J. Kleider is with General Dynamics C4 Systems, Scottsdale, AZ 85257, USA (e-mail: john.kleider@gdc4s.com).

This work was supported in part by the U. S. Army Research Laboratory under the Collaborative Technology Alliance Program, Cooperative Agreement DAAD19-01-2-0011 and in part by the National Science Foundation Graduate Research Fellowship Program.

Some results of this paper were presented at the IEEE International Conference on Acoustics, Speech, and Signal Processing, Honolulu, Hawaii, April 2007 [1].

Digital Object Identifier 10.1109/T-WC.2009.080065

$\mathbf{A}$, respectively; E[·] is the expectation operator; $\|\mathbf{x}\|_n$ is the ℓ_n norm of $\mathbf{x}$; $|\mathbf{x}|$ ($|\mathbf{A}|$) is a vector (matrix) that is the element-wise magnitude of $\mathbf{x}$ ($\mathbf{A}$); $\mathbf{A}^+ = (\mathbf{A}^{\mathcal{H}}\mathbf{A})^{-1}\mathbf{A}^{\mathcal{H}}$ is the pseudoinverse of matrix $\mathbf{A}$; $|\mathcal{A}|$ is the cardinality of set $\mathcal{A}$; $((\cdot))_N$ is the modulo N operation; int(·) rounds the argument to the nearest integer; $\mathbf{D}_{\mathbf{x}}$ is a diagonal matrix with vector $\mathbf{x}$ on the diagonal; $[\mathbf{A}]_{i,k}$ denotes entry in the ith row and the kth column of $\mathbf{A}$; finally, the $N \times N$ discrete Fourier transform (DFT) matrix is denoted by $[\mathbf{Q}]_{k,n} = N^{-1/2}\exp(-j2\pi(n-1)(k-1)/N),\ 1 \le k,n \le N$.

OFDM model: A PSAM OFDM system with null edge subcarriers is assumed in this paper. The pilot, null and data subcarrier indices can be grouped into three disjoint sets, $\mathcal{K}_p$, $\mathcal{K}_n$ and $\mathcal{K}_d$, respectively, that span all N baseband subcarriers indices. The frequency domain symbol is

$$\mathbf{x} = [x_1, x_2, ..., 0, 0, ..., 0, ..., x_{N-1}, x_N]^T, \tag{1}$$

where x_k is chosen to be a scaled version of an element from a finite constellation in the complex domain, $\mathcal{A} = \{a_1, a_2, ..., a_{|\mathcal{A}|}\}$ such that $\mathrm{E}\left[\|\mathbf{x}\|_2^2\right] = \mathcal{E}_s$, where $\mathcal{E}_s$ is the total transmitted symbol energy.

The received baseband frequency-domain signal after synchronization and cyclic prefix (CP) removal is

$$\mathbf{y} = \mathbf{D}_{\mathbf{h}}\mathbf{x} + \mathbf{w}, \tag{2}$$

where $\mathbf{w}$ is additive white complex Gaussian noise with autocovariance matrix $\sigma_w^2\mathbf{I}_N$ and $\mathbf{h}$ is the frequency response of the channel. Note that $\mathbf{h} = \mathbf{Q}_L\mathbf{h}^{(t)}$, where $\mathbf{h}^{(t)}$ is a length-L vector of the channel impulse response and $\mathbf{Q}_L$ is the first L columns of the DFT matrix $\mathbf{Q}$.

The received pilot subcarriers can now be expressed as

$$\mathbf{y}_p = \mathbf{D}_{\mathbf{h}_p}\mathbf{x}_p + \mathbf{w}_p. \tag{3}$$

Define $\mathbf{x}_p$ as a vector containing elements from $\mathbf{x}$ with indices in $\mathcal{K}_p$; vectors $\mathbf{y}_p$, $\mathbf{w}_p$ and $\mathbf{h}_p$ are similarly defined. Denote the portion of the DFT matrix that translates $\mathbf{h}^{(t)}$ to the pilot subcarriers by

$$\mathbf{Q}_p \triangleq [\mathbf{Q}]_{\mathcal{K}_p,\ \{1,2,...,L\}}, \tag{4}$$

so that $\mathbf{Q}_p \in \mathbb{C}^{|\mathcal{K}_p| \times L}$. Let $\mathbf{h}_p = \mathbf{Q}_p\mathbf{h}^{(t)}$.

Denote the channel estimate over the data subcarriers as $\hat{\mathbf{h}}_d$, which can be generated using the matrix

$$\mathbf{Q}_d \triangleq [\mathbf{Q}]_{\mathcal{K}_d,\ \{1,2,...,L\}}, \tag{5}$$

so that $\mathbf{Q}_d \in \mathbb{C}^{|\mathcal{K}_d| \times L}$. Let $\hat{\mathbf{h}}_d = \mathbf{Q}_d\hat{\mathbf{h}}^{(t)}$. The transmitted constellation points can be estimated by

$$\hat{\mathbf{x}}_d = \arg\min_{\mathbf{a} \in \mathcal{A}^{|\mathcal{K}_d|}} \left\| \mathbf{y}_d\mathbf{D}_{\mathrm{E}[|\mathbf{x}_d|^2]}^{-1/2} - \hat{\mathbf{h}}_d\mathbf{a} \right\|_2, \tag{6}$$

where $\mathcal{A}^{|\mathcal{K}_d|}$ is a $|\mathcal{K}_d|$ dimensional vector space containing elements from the set $\mathcal{A}$. Define $\mathbf{x}_d$ as a vector containing elements from $\mathbf{x}$ with indices in $\mathcal{K}_d$; vectors $\mathbf{y}_d$ and $\mathbf{h}_d$ are similarly defined. Implicit in (6) is that the accuracy of the channel estimate only matters in the data subcarriers. In other words, the accuracy of $[\hat{\mathbf{h}}]_k$ for $k \notin \mathcal{K}_d$ is irrelevant as it does not effect the data symbol estimation performance.

II. Channel Estimation

The procedure used to estimate the channel in a PSAM OFDM system varies depending on a number of factors including computational resources and knowledge of the channel statistics. In this paper, we examine least-squares error (LSE) channel estimation, which requires no knowledge of the channel statistics and treats the channel taps as unknown deterministic variables. It was shown in [6] that LSE estimation achieves the Cramér-Rao bound. When some knowledge of the channel statistics is available, it is possible to use more accurate equalizer structures such as Bayesian channel estimation [21, p. 532], but this increased accuracy comes at the expense of higher complexity and increased overhead. Methods have been proposed to reduce the complexity of Bayesian channel estimation [22], [23], but LSE estimation is still desirable for cases when the channel autocovariance matrix is unknown. Also, other more complicated two-dimensional channel estimation techniques are possible that incorporate the time variations in the channel, see [24], [25]. In this paper, we focus on the problem of channel estimation for null-subcarrier OFDM using pilots and an LSE estimator and assume the channel is approximately constant over one OFDM symbol, but can change from symbol to symbol.

If the channel statistics are unknown, then the channel impulse response can be treated as an unknown length-L deterministic vector[1]. The goal of channel estimation is to estimate this vector with as much accuracy as possible. By rewriting (3) as $\mathbf{y}_p = \mathbf{D}_{\mathbf{x}_p}\mathbf{Q}_p\mathbf{h}^{(t)} + \mathbf{w}_p$ and using the definition of $\mathbf{h}_d$, we can show that the LSE of the channel response in the data subcarriers is [21, p. 523],

$$\begin{aligned} \hat{\mathbf{h}}_d &= \underbrace{\mathbf{Q}_d\left(\mathbf{Q}_p^{\mathcal{H}}\mathbf{D}_{\mathbf{x}_p}^{\mathcal{H}}\mathbf{D}_{\mathbf{x}_p}\mathbf{Q}_p\right)^{-1}\mathbf{Q}_p^{\mathcal{H}}\mathbf{D}_{\mathbf{x}_p}^{\mathcal{H}}}_{\mathbf{P}}\mathbf{y}_p \\ &= \mathbf{h}_d + \mathbf{P}\mathbf{w}_p. \end{aligned} \tag{7}$$

Similar to [4], in this paper we require the number of pilots be at least the length of the channel impulse response vector i.e. $|\mathcal{K}_p| \ge L$. In LSE estimation, if this condition is not met, then the channel estimate in (7) will not be unique because the system of equations will be under-determined.

Notice that this estimate in (7) does not require $\mathbf{x}_p$ to be drawn from any specific constellation. Instead, the requirement is that the receiver know the pilots sent by the transmitter so that $\mathbf{D}_{\mathbf{x}_p}$ and $\mathbf{Q}_p$ can be generated from the complex values modulating $\mathbf{x}_p$ and the positions of the pilots $\mathcal{K}_p$, respectively. Furthermore, the complexity of this estimator is not dependent on the values of $\mathbf{x}_p$ or $\mathcal{K}_p$. All that is required is that the pilot design, as specified completely by $\mathbf{x}_p$ and $\mathcal{K}_p$, be known to both the transmitter and receiver.

[1]Strictly speaking the channel impulse response is only an approximation of the time-domain channel function. When the multipath impulses do not fall in the discrete sampling grid, the channel impulse response function will be infinite length and can not be captured with an length-L vector [26]. A discrete cosine transform-based method has been proposed to mitigate this problem in [27]. Also, in [28] a method was presented to resample a multipath profile so that it contains a finite number of channel taps after resampling while preserving the RMS delay spread of the channel. In this work, we assume that the tails of the impulse response function are negligible beyond L samples, which is also the assumption made in OFDM to justify that no ISI occurs.

Define the channel estimation error, $\boldsymbol{\zeta} \triangleq \hat{\mathbf{h}}_d - \mathbf{h}_d = \mathbf{P}\mathbf{w}_p$. It is straightforward to obtain its autocovariance matrix as

$$\begin{aligned}\mathbf{R}_{\boldsymbol{\zeta}} &= \mathrm{E}\left[\mathbf{P}\mathbf{w}_p\mathbf{w}_p^{\mathcal{H}}\mathbf{P}^{\mathcal{H}}\right] \\ &= \sigma_w^2\mathbf{Q}_d\left(\mathbf{Q}_p^{\mathcal{H}}\mathbf{D}_{\mathbf{x}_p}^{\mathcal{H}}\mathbf{D}_{\mathbf{x}_p}\mathbf{Q}_p\right)^{-1}\mathbf{Q}_d^{\mathcal{H}}. \end{aligned} \quad (8)$$

Of interest are the diagonal elements of the autocovariance matrix, $\mathbf{z} \triangleq \mathrm{diag}\{\mathbf{R}_{\boldsymbol{\zeta}}\}$, as they correspond to the variance of the channel estimate in each of the data subcarriers.

A. Data Subcarrier Estimation MSE

Using the criterion in (6), the metric that quantifies the data symbol estimation error is

$$\boldsymbol{\epsilon} \triangleq \mathbf{D}_{\mathrm{E}[|\mathbf{x}_d|^2]}^{-1/2}(\mathbf{y}_d - \mathbf{D}_{\hat{\mathbf{h}}_d}\mathbf{x}_d). \quad (9)$$

When the LSE channel estimates are used, $\boldsymbol{\epsilon}$ conditioned on $\mathbf{x}_p$ is complex Gaussian distributed with zero mean and autocovariance matrix

$$\mathbf{R}_{\boldsymbol{\epsilon}} = \mathbf{D}_{\mathbf{z}} + \sigma_w^2\mathbf{D}_{\mathrm{E}[|\mathbf{x}_d|^2]}^{-1}, . \quad (10)$$

Define $\mathbf{e} \triangleq \mathrm{diag}\{\mathbf{R}_{\boldsymbol{\epsilon}}\}$.

The probability of bit error is a function of some norm of $\mathbf{e}$ that is dependent on the channel statistics. In the following analysis we use an objective function that is the ℓ_∞ norm of $\mathbf{e}$, $\|\mathbf{e}\|_\infty$, but the optimization can easily be extended to any convex norm of $\mathbf{e}$, including the frequently-used ℓ_2 norm, by simply redefining the objective function. Using the ℓ_∞ in the objective function has the advantage that the optimized pilot placement will produce a constant channel estimate error across all data subcarriers. For the case where there are no null subcarriers, the optimal equal-spaced pilot placement is MSE-optimal in both the ℓ_2 and ℓ_∞ norms because it produces a constant channel estimate performance across all subcarriers. A good comparison of various MSE objective function norm choices can be found in [29]. Later, in Section IV, we illustrate how the performance is affected by the choice of the objective function norm.

Thus, the optimization problem that needs to be solved is

$$\begin{aligned}\arg\min_{\mathrm{E}[|\mathbf{x}|^2],\ \mathcal{K}_p} \quad & \|\mathbf{e}\|_\infty \\ \text{subject to} \quad & \mathrm{E}\left[\|\mathbf{x}\|_2^2\right] = \mathcal{E}_s, \\ & \mathbf{x}_n = \mathbf{0}_{|\mathcal{K}_n|\times 1}. \end{aligned} \quad (11)$$

In other words, the optimization variables are the distribution of power among the non-zero subcarriers $\mathrm{E}[|\mathbf{x}|^2]$, the power allocated to the pilots[2] and the positions of the pilot subcarriers $\mathcal{K}_p$, which along with $\mathcal{K}_n$ dictate the positions of the data subcarriers $\mathcal{K}_d$. The constraints are that the total symbol power be bounded by $\mathcal{E}_s$ and that the null subcarriers are set to zero. The objective function is discontinuous in the optimization variable $\mathcal{K}_p$. Therefore (11) is a non-convex optimization problem which is difficult to solve [30]. Next we propose to parameterize the pilot spacings and employ convex optimization techniques to produce a near optimal solution to (11).

[2]It is assumed that the power in the pilot subcarriers is deterministic, so that $\mathrm{E}\left[|\mathbf{x}_p|^2\right] = |\mathbf{x}_p|^2$.

III. LSE Pilot Design

In order to simplify the optimization problem in (11), we propose that it be split into two independent optimization problems that can be solved successively to find a near-optimal solution to (11): i) find a set of pilot subcarrier indices, $\mathcal{K}_p$, that make practical sense; ii) using this $\mathcal{K}_p$ as an additional constraint in (11), minimize the symbol estimate MSE, $\mathbf{e}$.

A. Pilot Position Parametrization

For small values of $|\mathcal{K}_p|$ and $N - |\mathcal{K}_n|$, it may be possible to exhaustively search all the possibilities of $\mathcal{K}_p$ to find the one that solves (11). But when $|\mathcal{K}_p|$ and $N - |\mathcal{K}_n|$ become moderately large, searching the $\binom{N-|\mathcal{K}_n|}{|\mathcal{K}_p|}$ possibilities of $\mathcal{K}_p$ becomes intractable. For instance, with $N - |\mathcal{K}_n| = 192$ and $L = 16$, $\binom{192}{16} \approx 10^{23}$.

Our goal is to limit the search space for $\mathcal{K}_p$ to only a relatively small number of reasonable possibilities. To do this, we propose to parameterize the pilot positions by a cubic polynomial. Note that equal pilot spacing implies that the pilot positions are described by a linear function, i.e., a first order polynomial. Thus, to allow unequal pilot spacing and to ensure a certain degree of parsimony, it is reasonable to consider parametric modeling of the pilot spacing using other low order polynomials. It is desirable to have the pilots symmetric with respect to the center of the band - this requirement rules out the quadratic polynomial design since a second order polynomial cannot be symmetric. A cubic polynomial parameterization is therefore the next logical design.

First, we need to find a one-to-one mapping that relates the set of indices $\mathcal{K}$ to the set of "subcarrier numbers" $\mathcal{S}$, where $\mathcal{S}$ is a circularly shifted version of $\mathcal{K}$ with a domain in the integers of $[-N/2+1, N/2]$. Specifically, $\mathcal{S} = f(\mathcal{K})$ where

$$f(\mathcal{K}) \triangleq ((\mathcal{K} - N + 1))_N - N/2 + 1. \quad (12)$$

If the domain of f is restricted to $[1, N]$, then f is a one-to-one mapping so that $\mathcal{K} = f^{-1}(\mathcal{S})$. With $\mathcal{S}$, the data and pilot subcarrier numbers, $\mathcal{S}_d \bigcup \mathcal{S}_p$, are continuous over the integers (this is not the case with $\mathcal{K}$ because the null indices $\mathcal{K}_n$ occupy the middle segment of $\mathbf{x}$).

The goal is to find a cubic function, $g(\cdot)$, that maps the integers in $[0, |\mathcal{K}_p| - 1]$ to a set of possible pilot subcarrier numbers, $\mathcal{S}_p$. Once $\mathcal{S}_p$ is found through $g(\cdot)$, we can use $f^{-1}(\cdot)$ to find $\mathcal{K}_p$ and finally, use $\mathcal{K}_p$ to solve the segmented optimization problem discussed at the beginning of Section III. This process will be performed iteratively over all permissible values of

$$\mathcal{K}_p = \left\{\mathrm{int}\left(f^{-1} \circ g(\tau)\right) \middle| \tau \in \{0, 1, 2, ..., |\mathcal{K}_p| - 1\}\right\} \quad (13)$$

until the minimizing set is found. The cubic function that parameterizes the pilot subcarrier positions has the form

$$g(\tau) = a_3\tau^3 + a_2\tau^2 + a_1\tau + a_0. \quad (14)$$

The pilots have to be placed in a non-null subcarrier (i.e. an in-band subcarrier). We further constrain $g(\tau)$ by assuming that the pilots are placed symmetrically about the center of the in-band region. Moreover, we assume that the pilots are placed sequentially from left to right, i.e., $g(\tau)$ has a positive slope. To further explain these constraints, let us define the

number of in-band subcarriers, $N_i \triangleq |\mathcal{S}_p \bigcup \mathcal{S}_d|$. It is necessary to have $\text{int}\left(f^{-1} \circ g(\tau)\right) \notin \mathcal{K}_n$, which means $g(\tau) \in [-(N_i - 1)/2, (N_i+1)/2]$. The middle of the in-band region is at $1/2$. Mathematically, the constraint equations are

$$g\left(\frac{|\mathcal{K}_p| - 1}{2}\right) = 1/2 \quad (15)$$

$$g(0) = -(N_i - 1)/2 + \delta \quad (16)$$

$$g(|\mathcal{K}_p| - 1) = (N_i + 1)/2 - \delta \quad (17)$$

$$g'(\tau) > 0, \quad (18)$$

In the constraint equations, δ represents how far the edge pilots are from the in-band edges. For example, $\delta \in (0, 1]$ would mean the edge pilots are placed at the in-band edge, while $\delta \in (1, 2]$, would place the edge pilots one subcarrier from the in-band edge. Using the constraint equations in (15)-(18) and the fact that the edge pilots should not be spaced further from the in-band edge than the average pilot spacing, it is possible to eliminate three of the five variables and define a domain of the remaining two variables so that

$$a_0 = \delta - \frac{(N_i - 1)}{2} \quad (19)$$

$$a_1 = \frac{a_3(|\mathcal{K}_p| - 1)^3 + 2N_i - 4\delta}{2(|\mathcal{K}_p| - 1)} \quad (20)$$

$$a_2 = \frac{-3a_3(|\mathcal{K}_p| - 1)}{2} \quad (21)$$

$$\frac{-2(N_i - 2\delta)}{(|\mathcal{K}_p| - 1)^3} \leq a_3 \leq \frac{4(N_i - 2\delta)}{(|\mathcal{K}_p| - 1)^3} \quad (22)$$

$$0 < \delta \leq \frac{N_i}{|\mathcal{K}_p|}. \quad (23)$$

From (21), when $a_3 = 0$, $a_2 = 0$ as well; which means that $g(\tau)$ in (14) becomes a first order polynomial and the pilot spacing becomes even. From (14) and (21), we infer that

$$g''(\tau) = 6a_3\tau + 2a_2 \quad (24)$$

$$= 6a_3\left(\tau - \frac{|\mathcal{K}_p| - 1}{2}\right). \quad (25)$$

Therefore, when $a_3 < 0$, pilot spacing increases as τ goes from 0 to $\frac{(|\mathcal{K}_p|-1)}{2}$, meaning that the pilot spacing at the edges of the in-band region are more closely spaced than the pilots in the middle of the in-band region. Conversely, when $a_3 > 0$ the outer pilots have a larger spacing than the pilots near the middle of the in-band region. Based on the results from [6], it is expected that $a_3 < 0$ will produce better pilot designs than $a_3 > 0$, which will be confirmed in Section IV of this paper. Fig. 1 is a plot of three example pilot parameterizations. In the plot the function $g(\tau)$ is plotted for different scenarios of a_3. The dots on each line indicate where the pilots would be placed.

B. Pilot Power

Assume that a set of plausible pilot indices generated with the cubic parametrization procedure from the last subsection is $\mathcal{K}_p$. If $|\mathcal{K}_p| = L$, i.e. $\mathbf{Q}_p$ as in (4) is square, then it is possible to write

$$\mathbf{z} = \text{diag}\left\{\sigma_w^2 \mathbf{Q}_d \mathbf{Q}_p^{-1} \mathbf{D}_{|\mathbf{x}_p|^{-2}} \mathbf{Q}_p^{\mathcal{H}^{-1}} \mathbf{Q}_d^{\mathcal{H}}\right\}. \quad (26)$$

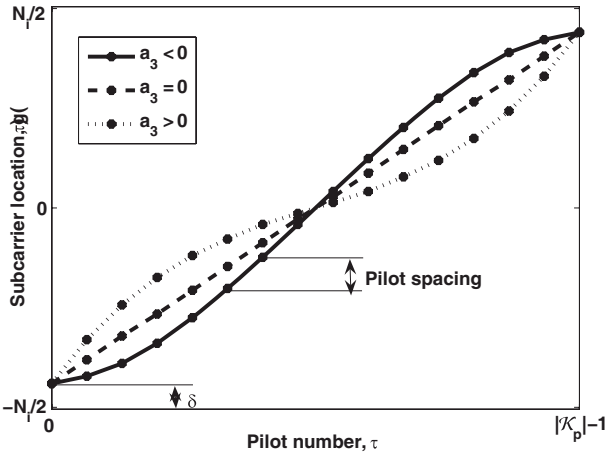

Fig. 1. Plot of pilot subcarrier position for different values of a_3.

When $|\mathcal{K}_p| > L$, (26) can be rewritten using pseudoinverses as

$$\mathbf{z} = \text{diag}\left\{\sigma_w^2 \mathbf{Q}_d \mathbf{Q}_p^{+} \mathbf{D}_{|\mathbf{x}_p|^{-2}} \mathbf{Q}_p^{\mathcal{H}^{+}} \mathbf{Q}_d^{\mathcal{H}}\right\} \quad (27)$$

as long as the power in the pilot subcarriers are constant (i.e. $[|\mathbf{x}_p|]_k = C \ \forall k$). However, since the pilot power in each subcarrier is not necessarily the same, it is necessary to use the approximation

$$\mathbf{z} \approx \text{diag}\left\{\sigma_w^2 \mathbf{Q}_d \mathbf{Q}_p^{+} \mathbf{D}_{|\mathbf{x}_p|^{-2}} \mathbf{Q}_p^{\mathcal{H}^{+}} \mathbf{Q}_d^{\mathcal{H}}\right\}$$

$$= \sigma_w^2 \underbrace{\left|\mathbf{Q}_d \mathbf{Q}_p^{+}\right|^2}_{\mathbf{A}} \underbrace{|\mathbf{x}_p|^{-2}}_{\mathbf{u}}, \quad (28)$$

where $\left|\mathbf{Q}_d \mathbf{Q}_p^{+}\right|^2$ is the element-wise magnitude square of the matrix $\mathbf{Q}_d \mathbf{Q}_p^{+}$. From (28), it is clear that the channel estimate MSE, $\mathbf{z}$, is linear in $|\mathbf{x}_p|^{-2}$ (which is the element-wise exponentiation of the vector). The decomposition/expansion of the channel-estimate MSEs is a novel idea and allows the optimization problem to be convex. For instance, in order to find the pilot design that minimizes the maximum channel estimate MSE (or average channel estimate MSE, using the ℓ_2 norm), we need to assume that a plausible set of pilot subcarriers $\hat{\mathcal{K}}_p$ is found using the procedures from Section III-A. With $\hat{\mathcal{K}}_p$, the pilot powers can be found by solving

$$\begin{aligned} \arg\min_{\mathbf{u}} \quad & \|\mathbf{A}\mathbf{u}\|_\infty \\ \text{subject to} \quad & \sum_{k=1}^{|\mathcal{K}_p|} \frac{1}{[\mathbf{u}]_k} = \mathcal{E}_p, \\ & \mathcal{K}_p = \hat{\mathcal{K}}_p, \\ & [\mathbf{u}]_k > 0 \ \forall \ k, \end{aligned} \quad (29)$$

where $\mathcal{E}_p$ is the total power allocated to the pilots.

So far we have derived a method for determining the pilot positions and optimizing the pilot power to minimize the *channel* estimate MSE. Next, we consider an alternate objective function that is based on the *symbol* estimate MSE. First, let us review the two main drawbacks to considering the channel estimate MSE instead of the symbol estimate MSE: i) even with a channel estimate MSE minimizing design, the channel estimate MSEs will not be constant over all of the data

subcarriers, which means the symbol estimate MSE will differ from subcarrier to subcarrier causing a non-constant quality of service across subcarriers; ii) the pilot power embedding ratio

$$\beta = \frac{\|\mathbf{x}_p\|_2^2}{\|\mathbf{x}\|_2^2} \tag{30}$$

is not known. Neither of these drawbacks are an issue when there are no null subcarriers present because the evenly-spaced equi-power design in such a case guarantees a constant channel estimate MSE across the band and because the symbol estimate MSE minimizing β has been derived in [31]. Thus, when null subcarrier are present, we advocate using the symbol estimate MSE as the objective function to be minimized.

The additional free variable in the symbol estimate MSE design is the power allocated to the *data* subcarriers. As we will see in Section IV, by using the ℓ_∞ norm of the *symbol* estimate MSEs, we can produce an almost constant symbol estimate MSE over all of the data subcarriers.

C. Subcarrier Power

To extend the pilot power design to the full design, the symbol estimate MSE can be rewritten as

$$\mathbf{e} = \sigma_w^2 \left(\left| \mathbf{Q}_d \mathbf{Q}_p^+ \right|^2 |\mathbf{x}_p|^{-2} + \left(\mathrm{E}\left[|\mathbf{x}_d|^2 \right] \right)^{-1} \right). \tag{31}$$

by substituting (28) into (10). It is possible to further simplify (31) by defining a new matrix $\mathbf{B} \in \mathbb{R}^{|\mathcal{K}_d| \times N_i}$ and vector $\mathbf{v} \in \mathbb{R}^{N_i \times 1}$ such that

$$\begin{aligned} \mathbf{e} &= \sigma_w^2 \underbrace{\left[\begin{array}{cc} \left| \mathbf{Q}_d \mathbf{Q}_p^+ \right|^2 & \mathbf{I}_{|\mathcal{K}_d| \times |\mathcal{K}_d|} \end{array} \right]}_{\mathbf{B}} \underbrace{\left[\begin{array}{c} |\mathbf{x}_p|^{-2} \\ \left(\mathrm{E}\left[|\mathbf{x}_d|^2 \right] \right)^{-1} \end{array} \right]}_{\mathbf{v}} \\ &= \sigma_w^2 \mathbf{B}\mathbf{v}. \end{aligned} \tag{32}$$

From (32), it is now obvious that the symbol estimate MSE $\mathbf{e}$ is linear in the vector $\mathbf{v}$. Once the optimizing $\mathbf{v}^\star$ is found it is straight forward to find the optimizing subcarrier powers $\mathrm{E}\left[|\mathbf{x}|^2 \right]$.

Assume that a plausible set of pilot subcarriers $\hat{\mathcal{K}}_p$ is found using the procedures from Section III-A. Using this pilot subcarrier set, we can simplify the optimization problem in (11) to

$$\begin{aligned} \arg\min_{\mathbf{u}} \quad & \|\mathbf{B}\mathbf{v}\|_\infty \\ \text{subject to} \quad & \sum_{k=1}^{|\mathcal{K}_d|} \frac{1}{[\mathbf{v}]_k} = \mathcal{E}_s, \\ & \mathcal{K}_p = \hat{\mathcal{K}}_p, \\ & [\mathbf{v}]_k > 0 \ \forall \ k. \end{aligned} \tag{33}$$

This optimization problem is convex since the objective function is a convex norm of a linear function and the constraint space is convex, thus it can be solved numerically using existing convex optimization software packages.

Now, the basic design procedure, which will be detailed in the next sub-section, is to solve (33) for all 'feasible' pilot subcarrier sets, $\hat{\mathcal{K}}_p$. The design chosen will be the one that minimizes $\|\mathbf{e}\|_\infty$.

D. Pilot Design Procedure

The overall pilot design procedures can be viewed as a grid search over the domain of $(\delta,\ a_3)$. Recall that the domain of $(\delta,\ a_3)$ is defined in (22) and (23). The pilot design procedure is outlined as a psuedo-code algorithm below

1) Initialize $i = 1$.
2) Select $\delta^{(i)}$ and $a_3^{(i)}$ in the domain defined by (22) and (23) and find $\hat{\mathcal{K}}_p^{(i)}$ according to (13).
3) Use $\hat{\mathcal{K}}_p^{(i)}$ to construct $\mathbf{B}^{(i)}$ via (32).
4) Solve (33) for $\|\mathbf{e}^{(\mathbf{i})}\|_\infty = \sigma_x^2 \|\mathbf{B}^{(i)}\mathbf{u}^{(i)}\|_\infty$.
5) If $\overline{MSE} > \|\mathbf{e}^{(i)}\|_\infty$ or $i = 1$, set $\overline{MSE} = \|\mathbf{e}^{(i)}\|_\infty$ and $\bar{i} = i$.
6) If $i = i_{max}$, exit, else, set $i = i + 1$ and go to Step 2.

When the algorithm exits, the optimizing values are $\mathbf{e}^\star = \mathbf{e}^{(\bar{i})}$, $\mathcal{K}_p^\star = \hat{\mathcal{K}}_p^{(\bar{i})}$ and $\mathbf{v}^\star = \mathbf{v}^{(\bar{i})}$. With these values, it is straightforward to find $\mathcal{K}_d^\star$ using the definition of the subcarrier sets and $\mathrm{E}\left[|\mathbf{x}|^2 \right]^\star$ using the definition of $\mathbf{v}$ in (32). Notice that these 'optimal' values and sets will only be optimal among all cubic parameterizations of the pilot subcarriers and thus they may not be the globally optimal values. Nevertheless, the proposed solution is guaranteed to perform at least as well as the equi-spaced pilot design.

IV. Pilot Design Optimization Example

For an example pilot design using the proposed procedure consider an OFDM system with N total subcarriers and $N/8$ null subcarriers on each band edge for a total of $N/4$ null subcarriers. Thus there are $N_i = 3N/4$ in-band non-null subcarriers. This null subcarrier scenario is used for example purposes, but the scheme proposed in this paper works for any number of null subcarriers. Of these in-band subcarriers, the number of pilot subcarriers and the number of data subcarriers will be varied in the following simulation examples. For all simulations, convex optimization problems were solved using [32].

For the error rate simulations the channel is Rayleigh where each channel tap is i.i.d. complex Gaussian with zero mean and diagonal autocovariance matrix $[\mathbf{R}_{\mathbf{h}^{(t)}}]_{k,k} = Ae^{-0.1k}$, where $k \in \{1, 2, ..., L\}$ and A is a constant selected so that $\mathrm{trace}\{\mathbf{R}_{\mathbf{h}^{(t)}}\} = 1$. Each error rate plot was generated using 100,000 channel realizations. Also, the channel is assumed to be independent from symbol to symbol. Recall that the proposed pilot design procedure is ambivalent to the statistics of the channel because it is based on LSE channel estimation.

A. Pilot positions

For the first example we have provided a plot in Fig. 2 of the maximum MSE $\|\mathbf{e}\|_\infty$ over a range of normalized a_3 values, where the NMSE is the MSE normalized by the perfect channel state information (PCSI) MSE which results when the receiver has full knowledge of the channel. That is

$$NMSE = \frac{\|\mathbf{e}\|_\infty}{MSE_{PCSI}} \tag{34}$$

$$= \frac{\|\mathbf{e}\|_\infty |\mathcal{K}_d|}{\sigma_w^2 \mathcal{E}_s}. \tag{35}$$

In (34), MSE_{PCSI} is the MSE when no pilot energy is used; instead all energy is allocated to the data subcarriers.

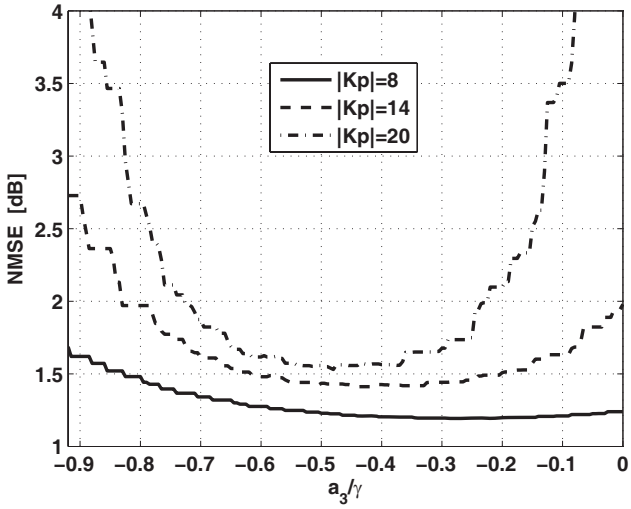

Fig. 2. Plot of maximum symbol estimate NMSE versus a_3/γ.

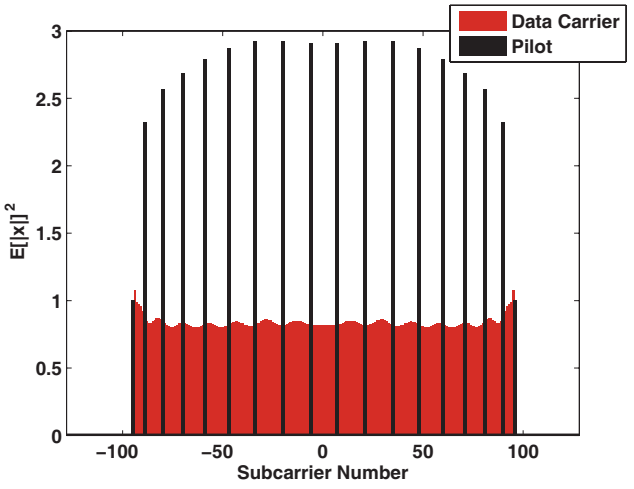

Fig. 3. Proposed design power spectrum density in linear scale.

In this case, the NMSE can be thought of as the penalty paid for channel estimation and by definition, the lower bound on NMSE will be 0dB.

The normalization factor for a_3 is

$$\gamma = \frac{2(N_i - 2\delta)}{(|\mathcal{K}_p| - 1)^3}, \tag{36}$$

which is the magnitude of the lower bound defined in (23). In the plot, $L = |\mathcal{K}_p|$. The resolution of the search grid was 0.01 in the δ dimension and 0.001 in the a_3 dimension. For all cases plotted, $|\mathcal{K}_n| > N/|\mathcal{K}_p|$, thus, as expected for the cases plotted, $\delta^\star = 0.01$. The lines plotted are precise and are not a result of simulation. The lack of smoothness in the lines comes from the fact that the maximum MSEs are a non-differentiable function of a_3.

In simulating Fig. 2, we compared the values of the MSE approximation in (28) and the true MSE from (8) which was used in the plot. We found that the difference between the two was always less than 0.1%, which indicates that for practical pilot scenarios, it is reasonable to use (28) in the pilot optimization objective function.

Symbol Power Profile: The PSD of the proposed design is plotted in linear scale in Fig. 3 where $N = 256$, $N_i = 192$ and $|\mathcal{K}_p| = L = 18$. With these parameters the proposed design has values $a_3 = -0.0371$ and $\delta = 0.01$. For both cases $\mathcal{E}_s = N_i$. Notice that for the proposed design the pilots near the band edges are spaced more closely together than the pilots near the middle of the band. Also, note that the power profile of the data subcarriers is not constant, but is instead chosen according to (33) so that the maximum symbol estimate MSE is minimized. A similar phenomenon occurs when $|\mathcal{K}_p| > L$. In the proposed scheme, the receiver would need to know how the data subcarrier power profile varies so that $\mathrm{E}[|\mathbf{x}_d|^2]$ can be determined and the data can be properly decoded. Because all of the proposed design procedures are performed off line and are channel ambivalent, it is straightforward to store the power values in memory. Finally, as was mentioned in the introduction, PAR is often a concern in OFDM systems. In OFDM it is not desirable to have samples in the time domain that have significantly higher power than the average sample, as this will increase PAR. In the proposed scheme, the power profile is being altered in the frequency domain. After these frequency domain pilots are mixed through the IFFT operation, they should not adversely effect the PAR. There is a comprehensive derivation of the PAR distribution based on the signal PSD in [33], which shows that the PAR distribution is not sensitive to slight PSD deviations from the ideal flat band-limited OFDM PSD. In fact, several papers have shown that, if the phases on these pilot subcarriers is carefully selected, it may be possible to reduce the PAR [14], [15], [34].

Cubic Coefficient Optimization: Fig. 4 is a plot of the optimizing values of a_3, $a_3^\star$, versus the ratio of pilot subcarriers to in-band subcarriers $|\mathcal{K}_p|/N_i$, where $|\mathcal{K}_p| = L$. The plot shows that the pilot spacing becomes more and more linear (i.e. a_3 approaches zero) as the number of pilot subcarriers increases. However, for all the values plotted, $a_3^\star$ is still negative which implies that the pilot carriers near the band edges should be more closely spaced than the center-band pilots.

Pilot Power Ratio: Fig. 5 is a plot of the ratio of pilot power to total power β defined in (30). Also plotted are the β values from [31],

$$\beta_{|\mathcal{K}_n|=0} = 1 - \frac{1}{1 + (N/L - 1)^{-1/2}} \tag{37}$$

which are MSE optimal when no null subcarriers are present. The plot demonstrates that for the null-subcarrier case, slightly more power should be allocated to the pilots than when all subcarriers are available. Thus, for the null subcarrier design the closed form expression in (37) should not be used.

Norm Choice & Channel Length Effect: So far, all of the simulations assume the channel length L is equal to the number of pilots, $|\mathcal{K}_p|$. This is the commonly used assumption when there is no channel state information. However, in practice, there may be scenarios when the channel length is known to be less than the number of pilots, that is, when $L < |\mathcal{K}_p|$. Ideally, the number of pilots should then be decreased to meet the channel length, but this is often not possible as the number of pilots are usually fixed as part of the communication standard. Despite this, it is possible to achieve some performance gains by using a value of L that is less than $|\mathcal{K}_p|$ in estimating the channel when it is known that the channel length does not exceed L.

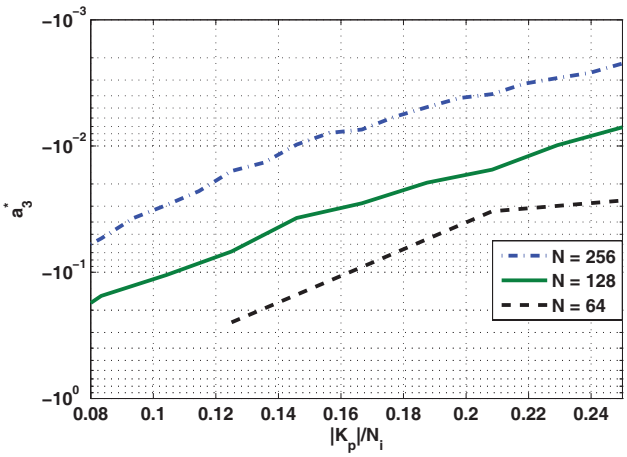

Fig. 4. Plot of MSE-optimizing values $a_3^\star$, $L = |\mathcal{K}_p|$.

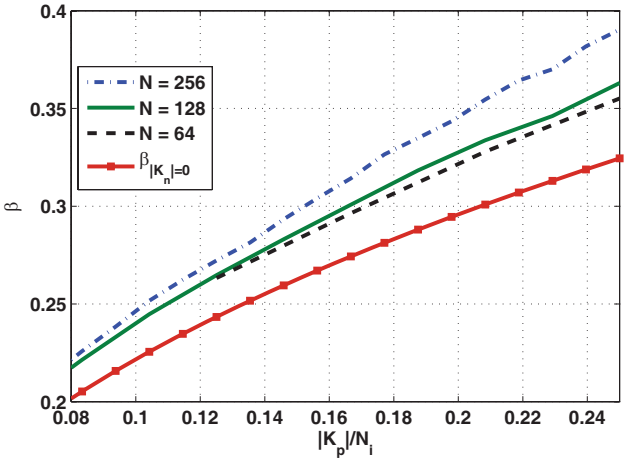

Fig. 5. Plot of β for the proposed design, $L = |\mathcal{K}_p|$.

The effect of this adjustment is plotted in Fig. 6 where the channel length L is varied for different numbers of pilots $L < |\mathcal{K}_p|$ where $N = 256$, $N_i = 192$. The plot shows that there will be some loss when more pilots are used than are needed. For example, the line corresponding $|\mathcal{K}_p| = 16$ has a lower (better) NMSE at L than either $|\mathcal{K}_p| = 28$ or $|\mathcal{K}_p| = 40$. This result is consistent with the equi-spaced pilot case, where in [4] a proof was provided showing that $|\mathcal{K}_p| = L$ minimizes the minimum ℓ_2 MSE. The plot also shows that the gap between the full-band equi-spaced pilot case where $N = N_i = 256$ is always less than 0.5dB. This can be considered the lower bound on the channel estimation performance as proved in [4].

Finally, the same plot also demonstrates the effect of using different norms in the objective function in (33). It is hard to distinguish the lines for the ℓ_∞ and ℓ_2 cases because they are almost equivalent. In fact, the difference is never greater than 0.01dB for all cases plotted. Such a narrow gap would imply that choosing one of these norms over the other is an unimportant choice. However, given the close performance gap slightly in favor of the ℓ_2 norm, the ℓ_∞ norm has the advantage of a constant quality of service over all subcarriers. The importance of having a constant MSE over all subcarriers varies with the application and channel code. The difference is probably only important when $|\mathcal{K}_p|$ is large, which causes the edge subcarriers to have much worse MSE than average

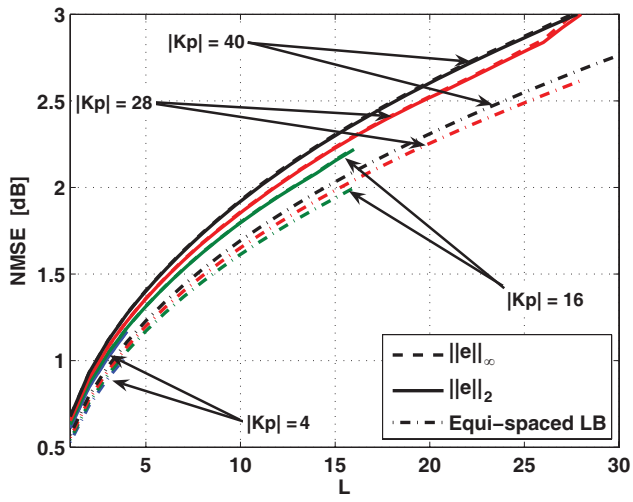

Fig. 6. NMSE for versus the channel length L for different numbers of pilots $|\mathcal{K}_p|$. For the equi-spaced lower bound, $|\mathcal{K}_n| = 0$.

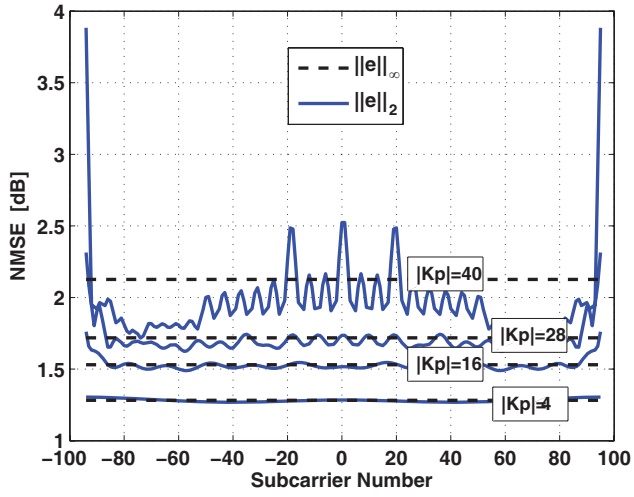

Fig. 7. NMSE for versus number of pilots $|\mathcal{K}_p|$ for the ℓ_2 and ℓ_∞ norms versus the subcarrier number. $L = |\mathcal{K}_p|$ in all cases.

when the ℓ_2 norm objective function is used. For comparison the NMSE across subcarriers is plotted in Fig. 7. For the $|\mathcal{K}_p| = 40$ case, the difference is about 2dB from the lowest NMSE subcarrier to the worst-case NMSE subcarrier near the band edge.

B. Comparisons

Typical Design: In order to assess the performance of the proposed pilot design, we chose to compare it to a "typical" pilot design named the "reference" design. For the reference design, $a_3 = 0$, $\beta = \beta_{|\mathcal{K}_n|=0}$ according to [31], all the pilots have a constant power and all of the data subcarriers have a constant power. Recall, that $a_3 = 0$ means that the pilots are evenly spaced in the in-band region. Also, for comparison, the pilot design proposed in [19] was generated. In [19], only the channel estimate MSE was considered, so to make the comparison fair, assume that all of the data subcarriers have constant power so that $\beta = \beta_{|\mathcal{K}|_n=0}$, which is MSE optimal for the full-band case.

The disadvantage of the design procedure in [19] is that it does not necessarily produce a viable pilot design. To

review, the pilot positions in [19] are chosen to be the $|\mathcal{K}_p|$ highest-power subcarriers from the preamble design. In general, this procedure works well because there are usually exactly $|\mathcal{K}_p|$ distinct high-power subcarriers in the preamble design. However, this characteristic of the preamble design is not guaranteed. As one example, when $N = 256$ and $|\mathcal{K}_p| = 10$ (or when $|\mathcal{K}_p| = 12$), the preamble design has spurious subcarriers in the center-band region that have higher power than the edge subcarriers. As a result the pilot design selected by the procedure in [19] has two adjacent pilots in the center-band region and no pilots at the edges of the in-band region, which produces catastrophic channel estimates. On the other hand, the design procedure proposed in this paper will always produce a reasonable pilot design.

This effect is illustrated in Fig. 8, which is a plot of the symbol estimate MSE versus the subcarrier number, where $N = 256$ and $|\mathcal{K}_p| = L = 10$. From the plot it is clear that the design from [19] does not allow for effective symbol estimation. In fact, the MSE performance is worse than that of the reference design. In comparison, the design proposed in this paper produces a flat MSE across all of the data subcarriers.

Fig. 9 is a plot of the MSE performance of the three designs when $N = 256$ and $|\mathcal{K}_p| = L = 18$. In this case, the design proposed in this paper and the design proposed in [19] have almost identical performance. On the other hand, the MSE for the reference design is very poor near the band edges. For perspective, we refer back to Fig. 3 and note that the proposed design results in non-uniform subcarrier spacing, especially in the vicinity of the null subcarriers. The resulting pilot power profile is distinctly non-equi-powered. Thus, although the proposed design in not dramatically non-uniform, Fig. 9 shows that the resulting performance gain in symbol NMSE is significant as compared to the conventional uniform-spacing design.

It should be pointed out that the design procedure in [19] may be somewhat less computationally complex than the procedure proposed in this paper. The reason being that many optimization problems (i.e. (33)) need to be solved over the bounded $(\delta,\ a_3)$ grid for the design in this paper. On the other hand, only two optimizations are necessary for the design procedure in [19]. Nevertheless, both designs can be determined in a matter of minutes and are meant to be performed only once offline. Thus, the computational complexity is not a prohibitive impediment for either scheme.

SER results: In Fig. 10 the uncoded symbol error rate (SER) of QPSK OFDM is plotted for the three pilot designs. For the plot, the Rayleigh fading channel described at the beginning of this section was used with $L = |\mathcal{K}_p|$. The SER performance of the proposed design is approximately 1dB worse than the PCSI case[3]. The plot also shows that the proposed design outperforms the reference design by about 1dB of SNR for the $L = 10$ case and more than 4dB of SNR for the $L = 18$ case. This performance gap is a result of the reference design having very poor channel estimates for the edge subcarriers. Finally, the design from [19] has almost identical performance

[3]In the PCSI case for this plot, $\beta = \beta_{|\mathcal{K}_n|=0}$ for the proposed pilot design. So despite PCSI, some energy is still allocated to the pilots, in order to make the comparisons realistic.

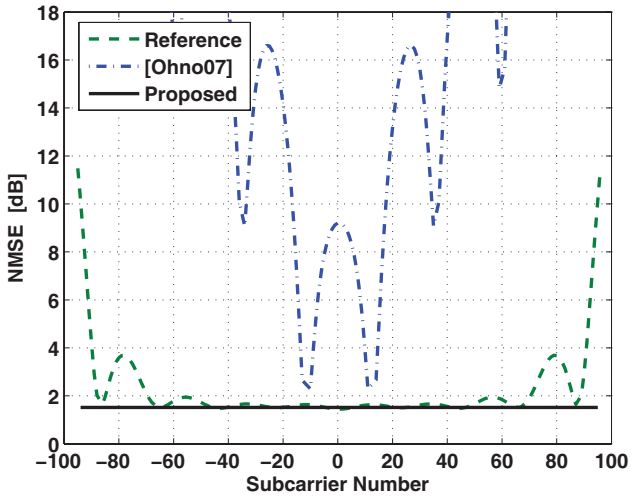

Fig. 8. MSE profile where $L = |\mathcal{K}_p| = 10$. $\delta = 5$ for the reference design.

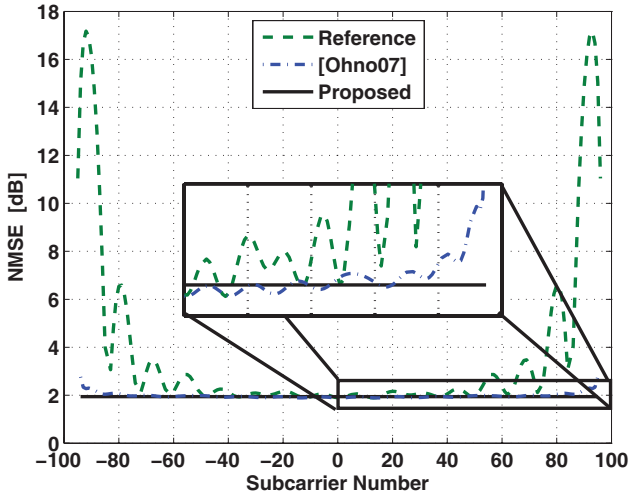

Fig. 9. MSE profile where $L = |\mathcal{K}_p| = 18$. $\delta = 0.01$ for the reference design.

as the proposed technique for the $L = 18$ case but is unusable for the $L = 10$ case.

IEEE 802.16 Improvement: In this subsection we explore the performance gains that could be realized if the pilots in IEEE 802.16 are rearranged according to the proposed design. The IEEE 802.16 standard contains three possible physical layer modes: Single carrier, OFDM, and orthogonal frequency division multiple access (OFDMA) [20]. Here, we focus only on the OFDM mode, but similar results can be realized for the other modes.

For IEEE 802.16 in OFDM mode [20, p. 427], the transmission frame is segmented into several parts. Of relevance here are the preamble and the data-carrying parts of the frame. The preamble is used for synchronization purposes including channel estimation. Additionally, each data-carrying symbol contains several pilots, which can be used for fine synchronization and also for channel estimation. In a data-carrying symbol 200 subcarriers of the 256 subcarrier window are used for data and pilots. Of the other 56 subcarriers, 28 are null in the lower-frequency guard band, 27 are nulled in the upper-frequency guard band and one is the DC subcarrier which is nulled. Of the 200 used subcarriers, 8 are

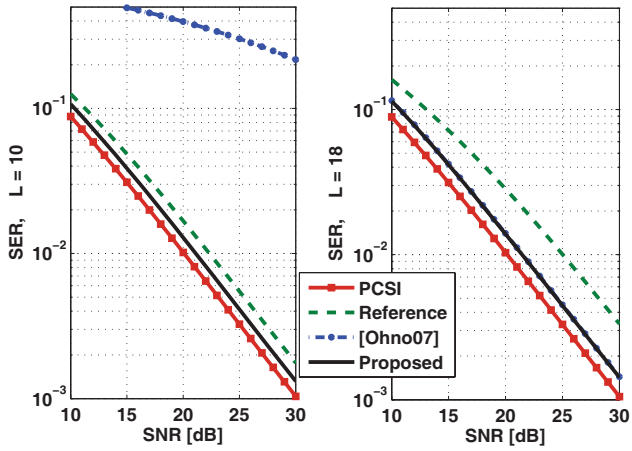

Fig. 10. SER performance, $L = |\mathcal{K}_p|$.

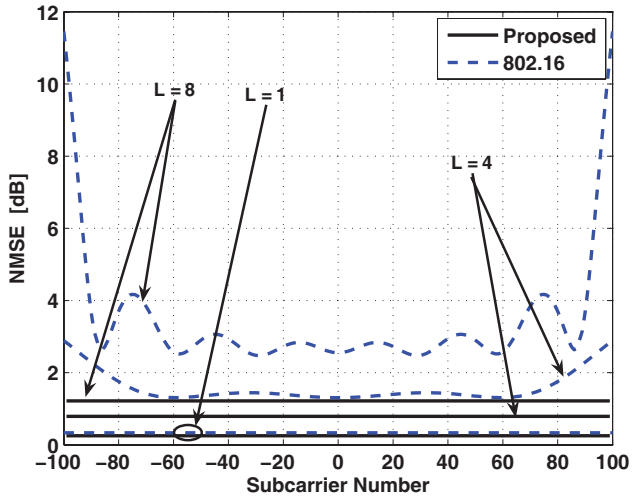

Fig. 11. NMSE performance of IEEE 802.16 versus the proposed design. $|\mathcal{K}_p| = 8$ in all cases.

allocated as pilots, while the remaining 192 are used for data transmission. The pilot positions specified by the standard are $\mathcal{K}_{p,OFDM} = \{-88, -63, -38, -13, 13, 38, 63, 88\}$, which all contain the same amount of power. Additionally, the pilot power ratio, β, is $\beta_{OFDM} = 1/25 = 0.04$. After solving the optimization problem in (33) using the 802.16 OFDM mode specifications, we find that $\hat{\mathcal{K}}_p = \{-100, -72, -43, -15, 15, 43, 72, 100\}$ for $L = 1$, $L = 4$ and $L = 8$ and that $\beta^{\star}_{L=1} = 0.067$, $\beta^{\star}_{L=4} = 0.124$ and $\beta^{\star}_{L=8} = 0.167$.

Fig. 11 is a plot of the NMSE of the proposed design and the 802.16 design. The plot shows that the standard pilot design does a poor job of estimating the symbols in the subcarriers near the guard band for $L > 1$. Conversely, the proposed pilot design is capable of a flat symbol estimate MSE across all data subcarriers.

Fig. 12, is a plot of the SER for the two pilot designs for different channel lengths using ideal interleaving and a (255, 239) Reed Solomon code as dictated by the 802.16 standard [20, p. 432]. The plot shows that, in an L-tap Rayleigh fading channel, the proposed pilot design leads to 3dB SNR improvement when $L = 8$ and a 1dB SNR improvement when $L = 4$.

All of the 802.16 results assume that the channel is estimated solely using the pilots in each symbol. In practice it may be possible to utilize the preamble symbol to help estimate the channel. However, in situations where the channel changes before the next preamble symbol is received, it is necessary to rely to the pilot aided channel estimates. In this case, as we have shown here, significant gains in 802.16 are possible with a simple reorganization of the pilots.

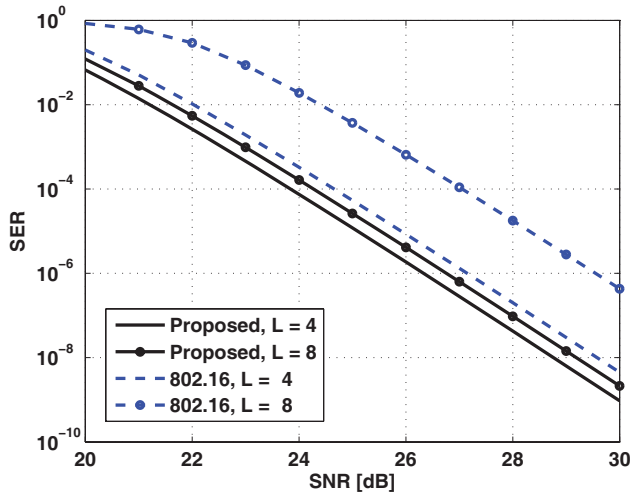

Fig. 12. Reed-Solomon coded SER performance of IEEE 802.16 versus the proposed design. $|\mathcal{K}_p| = 8$ in all cases.

V. Conclusions

In this paper we discussed the problem of channel estimation in null-subcarrier OFDM. Specifically, we presented an optimization method for designing pilots in a PSAM null-subcarrier OFDM system for the case when the channel statistics are unknown (LSE estimation). The proposed method utilizes a cubic polynomial to define the pilot spacing and convex optimization techniques to obtain the pilot and data powers such that the symbol-estimate MSE is minimized.

Through an example pilot design it was demonstrated that significant improvements in the symbol-estimate MSE and SER are possible with the proposed pilot design over the reference design. Also, when the proposed design procedure is applied to an IEEE 802.16 system operating in OFDM mode up to 3dB of coded BER improvement can be realized. For systems with more null subcarriers, even larger improvements are possible. In summary, for null-subcarrier OFDM systems where the channel statistics are unknown, large performance improvements can be realized by proper pilot design using the techniques proposed in this paper.

References

[1] R. J. Baxley, J. E. Kleider, and G. T. Zhou, "Pilot design for IEEE 802.16 OFDM and OFDMA," in *Proc. IEEE Intl. Conference on Acoustics, Speech and Signal Processing*, vol. 2, Apr. 2007.

[2] Z. Wang and G. Giannakis, "Wireless multicarrier communications," *IEEE Signal Processing Mag.*, vol. 17, pp. 29–48, June 2000.

[3] J. Cavers, "An analysis of pilot symbol assisted modulation for rayleigh fading channels," *IEEE Trans. Veh. Technol.*, vol. 40, pp. 686–693, Dec. 1991.

[4] R. Negi and J. Cioffi, "Pilot tone selection for channel estimation in a mobile OFDM system," *IEEE Trans. Consum. Electron.*, vol. 44, pp. 1122–1128, Sept. 1998.

[5] X. Cai and G. Giannakis, "Error probability minimizing pilots for OFDM with m-PSK modulation over Rayleigh-fading channels," *IEEE Trans. Veh. Technol.*, vol. 53, pp. 146–155, Feb. 2004.
[6] M. Morelli and U. Mengali, "A comparison of pilot-aided channel estimation methods for OFDM systems," *IEEE Trans. Signal Processing*, vol. 49, no. 12, pp. 3065–3073, 2001.
[7] E. Larsson and J. Li, "Preamble design for multiple-antenna OFDM-based WLANs with nullsubcarriers," *IEEE Signal Processing Lett.*, vol. 8, pp. 285–288, Dec. 2001.
[8] M. Dong, L. Tong, and B. Sadler, "Optimal pilot placement for channel tracking in OFDM," in *Proc. Military Communications Conference 2002*, pp. 602–606, Nov. 2002.
[9] H. Lo, D. Lee, and J. A. Gansman, "A study of non-uniform pilot spacing for PSAM," in *Proc. IEEE International Conference on Communications*, vol. 1, pp. 322–325, June 2000.
[10] S. Adireddy, L. Tong, and H. Viswanathan, "Optimal placement of training for frequency-selective block-fading channels," *IEEE Trans. Inform. Theory*, vol. 48, pp. 2338–2353, Aug. 2002.
[11] M. Dong and L. Tong, "Optimal design and placement of pilot symbols for channel estimation," *IEEE Trans. Signal Processing*, vol. 50, no. 12, pp. 3055–3069, 2002.
[12] C. Budianu and L. Tong, "Channel estimation for space-time orthogonal block codes," *IEEE Trans. Signal Processing*, vol. 50, pp. 2515–2528, Oct. 2002.
[13] X. Ma, L. Yang, and G. B. Giannakis, "Optimal training for MIMO frequency-selective fading channels," *IEEE Trans. Wireless Commun.*, vol. 4, pp. 453–466, Mar. 2005.
[14] R. J. Baxley and J. E. Kleider, "Embedded synchronization/pilot sequence creation using POCS," in *Proc. IEEE International Conference on Acoustics, Speech and Signal Processing, 2006.*, pp. 321–324, May 2006.
[15] R. Baxley, J. Kleider, and G. T. Zhou, "A method for joint peak-to-average power ratio reduction and synchronization in OFDM," in *Proc. IEEE Military Communicaitons Conference*, Oct. 2007.
[16] A. Aggarwal and T. H. Meng, "Minimizing the peak-to-average power ratio of OFDM signals using convex optimization," *IEEE Trans. Signal Processing*, vol. 54, pp. 3099–3110, Aug. 2006.
[17] L. Tong, B. Sadler, and M. Dong, "Pilot-assisted wireless transmissions: general model, design criteria, and signal processing," *IEEE Signal Processing Mag.*, vol. 21, pp. 12–25, Dec. 2004.
[18] H. Sari, G. Karam, and I. Jeanclaude, "Transmission techniques for digital terrestrial TV broadcasting," *IEEE Commun. Mag.*, vol. 33, pp. 100–109, Feb. 1995.
[19] S. Ohno, "Preamble and pilot symbol design for channel estimation in OFDM," in *Proc. IEEE International Conference on Acoustics, Speech and Signal Processing*, vol. 3, pp. 281–284, Apr. 2007.
[20] "IEEE standard for local and metropolitan area networks part 16: Air interface for fixed broadband wireless access systems," *IEEE Std 802.16-2004 (Revision of IEEE Std 802.16-2001)*, pp. 1–857, 2004.
[21] S. Kay, *Fundamentals of Statistical Signal Processing, Volume I: Estimation Theory*. Englewood Cliffs, NJ: Prentice-Hall, 1993.
[22] B. Yang, Z. Cao, and K. B. Letaief, "Analysis of low-complexity windowed DFT-based MMSE channel estimator for OFDM systems," *IEEE Trans. Commun.*, vol. 49, pp. 1977–1987, Nov. 2001.
[23] O. Edfors, M. Sandell, J. J. van de Beek, S. K. Wilson, and P. O. Borjesson, "OFDM channel estimation by singular value decomposition," *IEEE Trans. Commun.*, vol. 46, pp. 931–939, July 1998.
[24] Y. Li, L. J. Cimini, and N. R. Sollenberger, "Robust channel estimation for OFDM systems with rapid dispersive fading channels," *IEEE Trans. Commun.*, vol. 46, pp. 902–915, July 1998.
[25] F. Sanzi and J. Speidel, "An adaptive two-dimensional channel estimator for wireless OFDM with application to mobile DVB-t," *IEEE Trans. Broadcasting*, vol. 46, pp. 128–133, June 2000.
[26] J. J. van de Beek, O. Edfors, M. Sandell, S. K. Wilson, and P. O. Borjesson, "On channel estimation in OFDM systems," in *Proc. IEEE Vehicular Technology Conference*, vol. 2, pp. 815–819, July 1995.
[27] Y.-H. Yeh and S.-G. Chen, "DCT-based channel estimation for OFDM systems," in *Proc. IEEE International Conference on Communications*, vol. 4, pp. 2442–2446, June 2004.
[28] C. Mehlfhrer and M. Rupp, "Approximation and resampling of tapped delay line channel models with guaranteed channel properties," in *Proc. IEEE Intl. Conference on Acoustics, Speech and Signal Processing*, Apr. 2008.
[29] D. P. Palomar, J. M. Cioffi, and M. A. Lagunas, "Joint Tx-Rx beamforming design for multicarrier MIMO channels: a unified framework for convex optimization," *IEEE Trans. Signal Processing*, vol. 51, pp. 2381–2401, Sept. 2003.
[30] S. Boyd and L. Vandenberghe, *Convex Optimization*. Cambridge University Press, 2004.
[31] S. Ohno and G. B. Giannakis, "Optimal training and redundant precoding for block transmissions with application to wireless OFDM," *IEEE Trans. Commun.*, vol. 50, pp. 2113–2123, Dec. 2002.
[32] M. Grant and S. Boyd, "CVX: Matlab software for disciplined convex programming (web page and software)." http://stanford.edu/ boyd/cvx, March 2008.
[33] Q. Zhang, B. W. Han, J. H. Cho, and S. Wei, "PAPR performance of IDFT-based uncoded OFDM signals with null subcarriers and transmit filtering," in *Proc. IEEE International Conference on Communications*, vol. 10, pp. 4636–4641, June 2006.
[34] N. Chen and G. T. Zhou, "Superimposed training for OFDM: a peak-to-average power ratio analysis," *IEEE Trans. Signal Processing*, vol. 54, pp. 2277–2287, June 2006.

Robert J. Baxley is a Research Engineer with the Georgia Tech Research Institute (GTRI) Information Technology and Telecommunications Lab (ITTL). He received the B.S. degree in 2003, the M.S. degree in 2005, and the Ph.D. degree in 2008, all in Electrical Engineering from Georgia Tech. In 2005, Dr. Baxley received the institute-wide Sigma Xi award for best M.S. thesis and he is a recipient of the National Science Foundation Graduate Research Fellowship. His current research interests include communications theory, signal processing, and statistics.

John E. Kleider (M'95) received his B.S. degree in electrical engineering from University of Nebraska, Lincoln in 1985 and his M.S. degree in communications signal processing in 1993 from NTU, Fort Collins, CO.

He has been with General Dynamics in Scottsdale, Arizona working with high data rate and spread-spectrum communications since 2001. From 1994 to 2001 and from 1986 to 1990 he was with Motorola Government Electronics Group working in radar and communications. From 1990 to 1994 he was with Motorola Semiconductor. He has received awards for innovative technology from both General Dynamics and Motorola and has published numerous IEEE technical papers and has over 24 issued and pending U.S. and International patents. For the past six years he has been Principal Investigator leading a group of academic and industry partners addressing challenging communication issues for the U.S. Government. His current work includes many areas of communications and signal processing, including signal synchronization/diversity, channel estimation, equalization, OFDM, LPD/LPI waveform synthesis and analysis, RF watermarking, differential/coherent MIMO, VBLAST modulation, QoS-based multi-carrier adaptive modulation, multimedia joint source-channel-modulation coding, speaker identification, and noise reduction for speech recognition.. Presently he is conducting work in multiple transmitter synchronization, power efficient OFDM modulation, channel estimation, differential modulation, and MIMO communications. Mr. Kleider is a member of Eta Kappa Nu and Tau Beta Pi.

G. Tong Zhou received the B.Sc. degree in biomedical engineering and instrumentation from the Tianjin University, China, in 1989 and the M.Sc. degree in biophysics, the M.Sc. degree in electrical engineering, and the Ph.D. degree in electrical engineering, all from the University of Virginia (UVA), Charlottesville, in 1992, 1993, and 1995, respectively. Since September 1995, she has been with the School of Electrical and Computer Engineering at Georgia Tech, Atlanta, where she is now a Professor. Her research interests are in the general areas of statistical signal processing and communications applications. Dr. Zhou received the National Science Foundation Faculty Early Career Development (CAREER) Award in 1997. She served as Chair of the IEEE Signal Processing Society Signal Processing Theory and Methods Technical Committee during 2006 and 2007.